Chinese Journal of Oceanology and Limnology
Vol. 28 No. 3, P. 573-582, 2010
DOI: 10.1007/s00343-010-9062-x

Using genetic algorithms to calibrate a dimethylsulfide production model in the Arctic Ocean*

QU Bo (瞿波) [†,*], GABRIC J. Albert [††]
[†] *Nantong University, Nantong 226007, China*
[††] *Griffith University, Brisbane 4111, Australia*

Received Apr. 8, 2009; revision accepted July 9, 2009

Abstract The global climate is intimately connected to changes in the polar oceans. The variability of sea ice coverage affects deep-water formations and large-scale thermohaline circulation patterns. The polar radiative budget is sensitive to sea-ice loss and consequent surface albedo changes. Aerosols and polar cloud microphysics are crucial players in the radioactive energy balance of the Arctic Ocean. The main biogenic source of sulfate aerosols to the atmosphere above remote seas is dimethylsulfide (DMS). Recent research suggests the flux of DMS to the Arctic atmosphere may change markedly under global warming. This paper describes climate data and DMS production (based on the five years from 1998 to 2002) in the region of the Barents Sea (30–35°E and 70–80°N). A DMS model is introduced together with an updated calibration method. A genetic algorithm is used to calibrate the chlorophyll-*a* (CHL) measurements (based on satellite SeaWiFS data) and DMS content (determined from cruise data collected in the Arctic). Significant interannual variation of the CHL amount leads to significant interannual variability in the observed and modeled production of DMS in the study region. Strong DMS production in 1998 could have been caused by a large amount of ice algae being released in the southern region. Forcings from a general circulation model (CSIRO Mk3) were applied to the calibrated DMS model to predict the zonal mean sea-to-air flux of DMS for contemporary and enhanced greenhouse conditions at 70–80°N. It was found that significantly decreasing ice coverage, increasing sea surface temperature and decreasing mixed-layer depth could lead to annual DMS flux increases of more than 100% by the time of equivalent CO_2 tripling (the year 2080). This significant perturbation in the aerosol climate could have a large impact on the regional Arctic heat budget and consequences for global warming.

Keyword: Arctic Ocean; dimethyl sulfide; mixed-layer depth; chlorophyll-*a*; dimethyl sulfoniopropionate

1 INTRODUCTION

Dimethylsulfide (DMS) is the main volatile sulfur released during the formation and decay of microbial ocean biota (Lovelock, 1972). Aerosols formed from the atmospheric conversion of DMS to sulfate and methanesulfonic acid can exert a climate cooling effect directly by scattering and absorbing solar radiation and indirectly by promoting the formation of cloud condensation nuclei and increasing the albedo of clouds, thus reflecting more solar radiation back into space (Charlson et al., 1987). DMS contributes about 1.5×10^{13} g of sulfur to the atmosphere annually (Gage et al., 1997), about half of the global biogenic input of sulfur to the atmosphere (Kiene et al., 1990). It has also been suggested that the biological consumption of DMS seems to be a more important factor than atmospheric exchange in controlling DMS concentrations in the ocean and hence its flux to the atmosphere.

The main source of DMS is dimethyl sulfoniopropionate (DMSP) (Kiene et al., 1990). DMSP is primarily synthesized by phytoplankton (Archer, 2002), mostly prymnesiophytes and dinoflagellates (Matrai et al., 1997). Matrai et al. (1997) also found that in Arctic waters the contribution of diatoms to water column budgets of DMSP and DMS was as significant as that of *Phaeocystis* and cannot be overlooked. DMS and its biogenic precursor DMSP are both phytoplankton metabolites (Gabric et al., 1999). DMSP occurs in particulate

* Supported by the Nantong University Research Funding (No. 09R02)
** Corresponding author: qubo62@gmail.com

(DMSPp) and dissolved (DMSPd) forms. They can both biodegrade by cleavage into DMS. The transformation of DMSP to DMS and the control of DMS accumulation in surface waters are intricately linked to food-web dynamics and physiochemical processes, including photochemical degradation, vertical mixing and sea-to-air flux (Archer et al., 2002). The biogeochemical cycle of DMS (Fig.1) begins with its precursor DMSP. The bacterial metabolism of DMSPd may be the major mechanism for DMS production in seawater (Dacey et al., 1998). The other processes affecting the turnover of DMS include DMS photolysis and DMSPp sedimentation and the bacterial consumption of DMS and DMSP.

At its maximal extent, sea ice covers over 80% of the Arctic Ocean; however the recent steady decline in ice cover may have affected phytoplankton dynamics and ocean circulation systems and hence have had a significant impact on the global climate. Researchers have begun to investigate Arctic aerosols (Levasseur et al., 1994; Leck et al., 1996; Marai et al., 1997; Gabric et al., 1999; Treffeisen et al., 2005; Serreze et al., 2006; Holland et al., 2006; Kloster et al., 2007; Moline et al., 2008). If sea ice loss is extensive, the abundance of ice algae that have especially high DMSP content in the hypersaline and low temperature (Kirst et al., 1991) will also diminish. Researchers have begun investigating the nature of the Arctic aerosols (Levasseur et al., 1994; Leck et al., 1996; Marai et al., 1997; Gabric et al., 1999; 2005) and the complex influence of marine biota on the aerosol climate is being slowly unraveled (Leck et al., 2004).

In this work we apply a genetic algorithm (GA) to calibrate a DMS production model for the period 1998–2002 based on chlorophyll-*a* (CHL) satellite data in the same study region. To investigate possible changes under warming, global circulation model (GCM) forcings are used with a calibrated DMS model to the predict sea-to-air flux of DMS for enhanced greenhouse conditions (from $1\times CO_2$ to $3\times CO_2$) in the zonal 70–80°N latitude band.

2 METHODS

2.1 Updated DMS model

The DMS model was first introduced by Gabric et al. (1993) and adapted to the ecological structure of the nitrogen-based plankton community model of

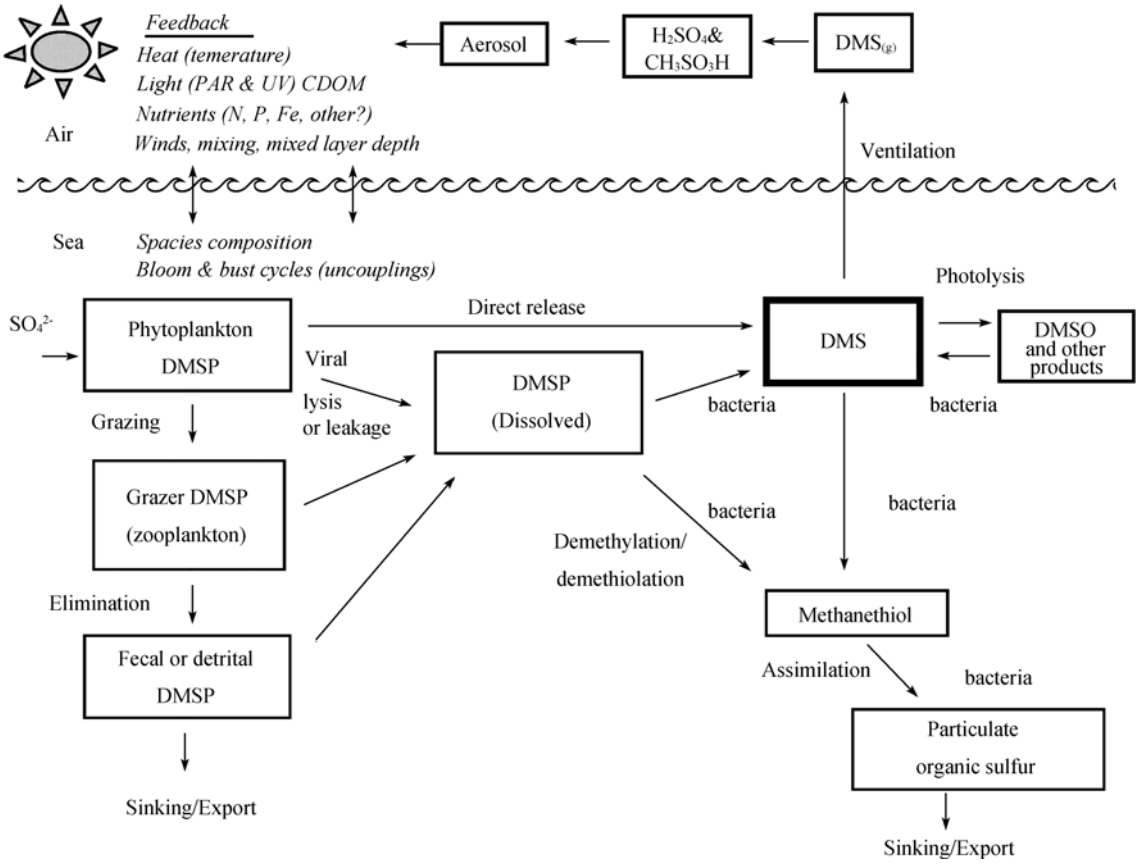

Fig.1 Schematic diagram of the major elements in DMS production and cycling

Moloney et al. (1986). The model is a depth-averaged model and was developed and applied for the subantarctic zone of the Southern Ocean (Gabric et al., 1998; 2002; 2003) and also used in a study of the Barents Sea (Gabric et al. 1999; 2005).

The DMS model used in this paper (see parameters listed in Table 1) is constructed using the following equations (detailed in Cropp, 2003).

Table 1 DMS model compartments

Compartments	Description
X1=P	Phytoplankton
X2=B	Bacteria
X3=F	Flagellates
X4=L	Large protozoa
X5=Z	Zooplankton
X6=N	Nitrogen (as nitrate)
X7=DMSP	Dimethyl sulfoniopropionate
X8=DMS	Dimethyl sulfide

$$\frac{\mathrm{d}P}{\mathrm{d}t} = k_{23}\left(\frac{N}{N+k_{24}}\right)P - k_4 PZ \tag{1}$$

$$\frac{\mathrm{d}Z}{\mathrm{d}t} = k_4(1-k_{20})PZ - k_{19}Z \tag{2}$$

$$\frac{\mathrm{d}N}{\mathrm{d}t} = k_{19}Z + k_4 k_{20} PZ - k_{23}\left(\frac{N}{N+k_{24}}\right)P \tag{3}$$

$$\frac{\partial DMSP}{\partial t} = k_5 P + k_{21} Z - k_{27} DMSP - k_{31} DMSP \tag{4}$$

$$\frac{\partial DMS}{\partial t} = k_6 P + k_{27} DMSP - k_{28} DMS - k_{29} DMS - k_{30} DMS \tag{5}$$

Here, the parameters K_i ($1<i<31$) are listed in Table 2 and P, Z, N are defined in Table 1, and they are based on data from stations 1 and 2 in the work of Gabric et al. (1999).

The change in DMS in the ocean is described by (Gabric et al. 2001)

$$\frac{\mathrm{d}DMS}{\mathrm{d}t} = F_{\mathrm{P}} + F_{\mathrm{DMSP}} - F_{\mathrm{B}} - F_{\mathrm{photo}} - F_{\mathrm{air}} \tag{6}$$

where F_{p} is the release of DMS from phytoplankton cells;

F_{DMSP} is the production of DMS from DMSP;

F_{B} is the loss of DMS due to bacterial consumption;

F_{photo} is the loss of DMS due to photolysis;

F_{air} is the loss of DMS due to emission to the atmosphere.

The ventilation of DMS to the atmosphere was calculated using the concentration of DMS produced in the mixed layer $\Delta C(=C_{\mathrm{O}}-C_{\mathrm{A}})$ and DMS sea-to-air transfer velocity K_w (Liss et al., 1986):

$$F_{\mathrm{air}} = K_w(C_{\mathrm{O}} - C_{\mathrm{A}}) \tag{7}$$

where C_{O} and C_{A} are the DMS concentrations in the ocean and atmosphere respectively. As the atmospheric concentration of DMS (C_{A}) is very small comparing with C_{O}, the sea-air flux of DMS can be approximated as

$$F_{\mathrm{air}} = K_w C_{\mathrm{O}} \tag{8}$$

where the transfer velocity K_w is mainly dependent on the sea surface temperature (SST) and wind velocity. The wind speed (w) is recorded 10 m above the sea surface. Gabric et al. (1995) rescaled K_w for DMS as follows:

$$\begin{aligned}
&K_w = 0.17(600/Sc)^{2/3} w && \text{for } w \le 3.6\\
&K_w = (600/Sc)^{1/2}(2.85w - 10.26) \\
&\quad + 0.612(600/Sc)^{2/3} && \text{for } 3.6 \le w \le 13\\
&K_w = (600/Sc)^{1/2}(5.9w - 49.91) \\
&\quad + 0.612(600/Sc)^{2/3} && \text{for } w > 13
\end{aligned} \tag{9}$$

Here, Sc is the temperature-dependent Schmidt number given by Erikson et al. (1990):

$$\begin{aligned}
Sc &= 2674.0 - 147.12 * SST \\
&\quad + 3.726 * SST^2 - 0.038 * SST^3
\end{aligned} \tag{10}$$

It should be noted that DMS ventilation can only occur in ice-free water. To account for this, the computed DMS transfer velocity was scaled by the percentage of ice-free water (Gabric et al. 1999).

3 RESULTS

3.1 DMS model calibration using a genetic algorithm

The characteristics of Barents Sea cruise data, satellite CHL data (mainly from SeaWiFS) and climatological data were described by Qu et al. (2006). The DMS model used (Eqs. 1–5) and the satellite and meteorological data for the CHL, SST, wind speed, cloud cover, photosynthetically active radiation and mixed-layer depth (MLD) were described in detail by Qu et al. (2006).

The GA is a non-derivative-based optimization technique first introduced by Holland (1975), and it provides a solution by mimicking evolution. The model calibration proceeds by minimizing the root-mean-squared difference between observations and model predictions through varying a subset of the most sensitive model parameters. The GA initializes a random sample of in silico individuals (typically 100 in number) with different randomly selected parameter values that define the parameter estimation problem. The evolution starts from a population of randomly generated individuals and proceeds in generations. In each generation, the fitness of each individual in the population is evaluated and multiple individuals are stochastically selected from the current population (based on their fitness) and modified (recombined and possibly randomly mutated) to form a new population. The selection scheme used is tournament selection with a shuffling technique for choosing random pairs for mating. The new population is then used in the next iteration of the algorithm. Iterations proceed until significant improvement in the overall fitness is no longer possible. The simplified DMS model is referred to as a subroutine of the genetic program that evaluates the population fitness function.

3.2 CHL calibration

The overall calibration proceeds in two stages with parameters affecting the surface chlorophyll prediction adjusted first and then those parameters that determine the DMS concentration. The six most sensitive parameters (determined in a previous analysis) were calibrated to the monthly mean CHL determined from SeaWiFS satellite data. The parameters are k_4, k_{19}, k_{20}, k_{23}, I_k and No. ($P + Z + N$). Model simulations were spun up for several years until a repeating annual cycle was achieved and subsequently run for one year starting from Julian day 1. CHL data are only available from 12th March to 27th September in SeaWiFS.

Parameter reference values derived in a previous Barents Sea study (Gabric et al. 1999) were used to initialize the parameter ranges for the GA runs. The monthly mean SST, wind speed, cloud cover, ice cover and MLD for each year are calculated and used to force the model. Fig.2 compares the calibrated model results and the original SeaWiFS CHL data for individual years (here, only results for 1998 and 1999 are shown) and the overall 5-year mean (1998–2002). The fitness values are quite low for the 5-year means (the closer to zero, the better the fit). The parameters (k_4, k_{19}, k_{20}, k_{23} and I_k) for the 1998–2002 calibration are listed in Table 3.

The results for the year 1998 have the best fit (-2.9), which is excellent, and those for the year 1999 (-4.1) and the mean of 1998–2002 (-4.4) also fit well. The results for the other years have a reasonable fit.

3.3 DMS calibration

Subsequent to the CHL calibration, the DMS specific parameters (gamma, k_{27}, k_{28}, k_{29} and k_{31}) were calibrated using the same GA algorithm. As there were limited observations of DMS in the Arctic, data for the precursor, DMSP, were taken from observations made during three cruises in the study

Table 2 Parameter values used in the DMS model

Parameter	Process	Unit
k_4	Z grazing rate on P	$m^3\,mgN^{-1}\,d^{-1}$
k_5	Release rate of DMSP by P	d^{-1}
k_6	Release rate of DMS by P	d^{-1}
k_{19}	Z specific N excretion rate	d^{-1}
k_{20}	Prop of N uptake excreted by Z	-
k_{21}	DMSP excretion rate by Z	d^{-1}
k_{23}	Maximum rate of N uptake by P	d^{-1}
k_{24}	Half-sat const for P uptake of N	$mgNm^{-3}$
k_{27}	DMSP-DMS conversion rate	d^{-1}
k_{28}	DMS consumption rate by B	d^{-1}
k_{29}	Max DMS photo-oxidation rate	d^{-1}
k_{30}	DMS ventilation rate to atmosphere	d^{-1}
k_{31}	DMSP consumption rate by B	d^{-1}
γ	Photoplankton S (DMSP):N ratio	-
I_k	Saturating light intensity for photosynthesis	Wm^{-2}
No=P+Z+N	Total nutrient	$mgNm^{-3}$

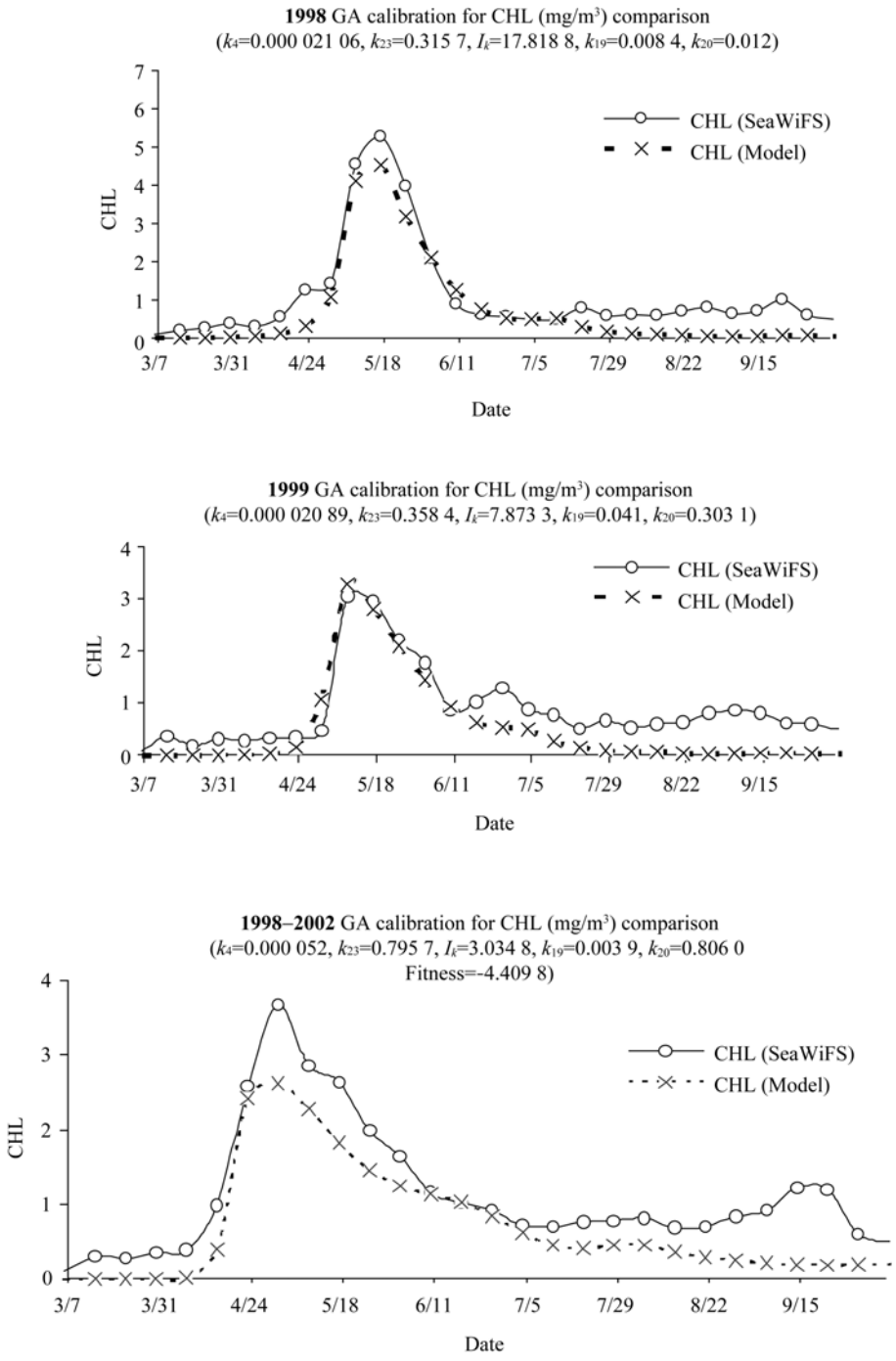

Fig.2 GA calibration results for CHL measurements at 70–80°N for 1998, 1999 and 1998–2002

Table 3 Main parameters in CHL GA calibrations

	1998–2002 fitness=-4.4	1998 fitness=-2.9	1999 fitness=-4.1	2000 fitness=-5.3	2001 fitness=-11.8	2002 fitness=-11.9
k_4	0.000 052 24	0.000 021 12	0.000 021 27	0.000 034	0.000 032	0.000 030
k_{19}	0.003 9	0.084	0.004 1	0.010 1	0.009 8	0.016 7
k_{20}	0.806 0	0.018 8	0.310 1	0.206 3	0.046 6	0.003 6
k_{23}	0.795 7	0.318 6	0.365 8	0.378 9	0.336 0	0.688 8
I_k	3.034 8	17.569 3	9.573 9	13.980 3	1.52	23.833 1
No	375.41	453.65	440.32	200.29	341.64	700.25

region (16 stations were sampled in March 1998, followed by 17 stations in May 1998 and 24 stations during June and July in 1999 (Matrai et al., 1997; Qu et al. 2006). Cubic spline interpolation was used to obtain values for April and June and the fitness function was calculated on the basis of March–July DMSP observation data (averaged over space and time). The resulting DMS calibrated parameters are given in Table 4.

4 DISCUSSION

Generally in the Barents Sea, the CHL bloom began in early April, gradually increased to its peak around the end of April or early May, and then decreased from the mid-May or June (Fig.2). From mid-June, the CHL decreased until it disappeared completely by the end of September. There was a second smaller bloom in September owing to the shoaling of the MLD in late summer. The concentration of surface CHL collected along the transect of the three cruises and the SeaWiFS satellite CHL data have been compared (Qu et al., 2006) and there was good agreement at most stations in the Barents Sea.

Zonal mean forcings at 70–80°N were obtained from a coupled climate model simulation using the Commonwealth Scientific and Industrial Research Organisation GCM (Gordon et al., 1997). Simulated forcings include the SST, wind speed, cloud cover, ice cover and MLD (Fig. 3 excludes the wind speed). A further CHL GA calibration was carried out using the zonal average SeaWiFS CHL data for 70–80°N during the 5-year period of 1998–2002. The excellent fitness value (-0.7 598) gives a new set of model parameter values. Those values are used for further simulation of the DMS flux perturbation.

The perturbation of the DMS flux under warming was derived using GCM outputs for the periods of 1960–1970 (pre-industry level, denoted as $1\times CO_2$) and 2078–2086 (triple equivalent CO_2 level, denoted as $3\times CO_2$), the levels of CHL, DMS, DMSP and zooplankton, and the DMS flux in ice-free water. Table 5 shows the GCM simulation results.

Fig.3 presents the monthly average values of the SST, cloud cover, ice cover and MLD for the two periods. The figure shows the SST is higher in autumn and lower in spring and early summer. The SST is expected to increase up to 2°C in its peak month of September and only 0.5°C in April. The wind speed does not change much overall but is higher in winter and spring and lower in summer. Cloud cover is high in winter and lower in summer (44% less for $1\times CO_2$ and 36% less for $3\times CO_2$ in June). Generally, cloud cover reduces by up to 19% in November by the period 2 078–2 086 and by 7.4% overall. Sea-ice cover reduces greatly over the next 80 years, especially during August–October, sea-ice would reduce up to 61%. The MLD decreases 6.5 m on average, with the shallowest period being September. The MLD is simulated to decrease 13% in May and 17% in July. The combination of the significant reduction in ice cover in autumn and a shallower MLD in summer results in the DMS flux increasing significantly in autumn over the next 80 years.

There is an empirical relation between the DMS flux, F_{DMS}, and the concentration of cloud condensation nuclei CCN (Lawrence, 1993):

$$CCN = 29F_{DMS} + 45 \quad (11)$$

Table 4 DMSP GA calibration in the study region for 1998–2002

	1998–2002	1998	1999	2000	2001	2002
k_{27}	0.275 1	0.275 1	0.103 0	0.275 1	0.275 1	0.275 1
k_{28}	0.111 5	0.111 5	0.151 9	0.111 5	0.111 5	0.111 5
k_{29}	0.442 1	0.442 1	0.032 9	0.442 1	0.442 1	0.442 1
k_{31}	0.254 1	0.254 1	0.054 1	0.254 1	0.254 1	0.254 1
γ	0.694 3	0.694 3	0.075 8	0.694 3	0.694 3	0.694 3

Table 5 GCM simulation results

	SST degC	Wind speed m/s	Cloud cover %	Ice cover %	MLD m	Peak CHL mg m^{-3}	DMS μmol m^{-2} d^{-1}	Z mgN m^{-3}	N mgN m^{-3}	DMS flux μmol m^{-2}
$1\times CO_2$	-0.24	4.2	82.1%	68.8%	41.8	2.9	12.1	0.8	0.25	0.8
$3\times CO_2$	0.71	4.5	74.7%	50.3%	35.3	2.5	13.1	1.7	0.3	1.8
Increased	40%	3%	-9%	-27%	-13%	-13.5%	8%	110%	21%	117%

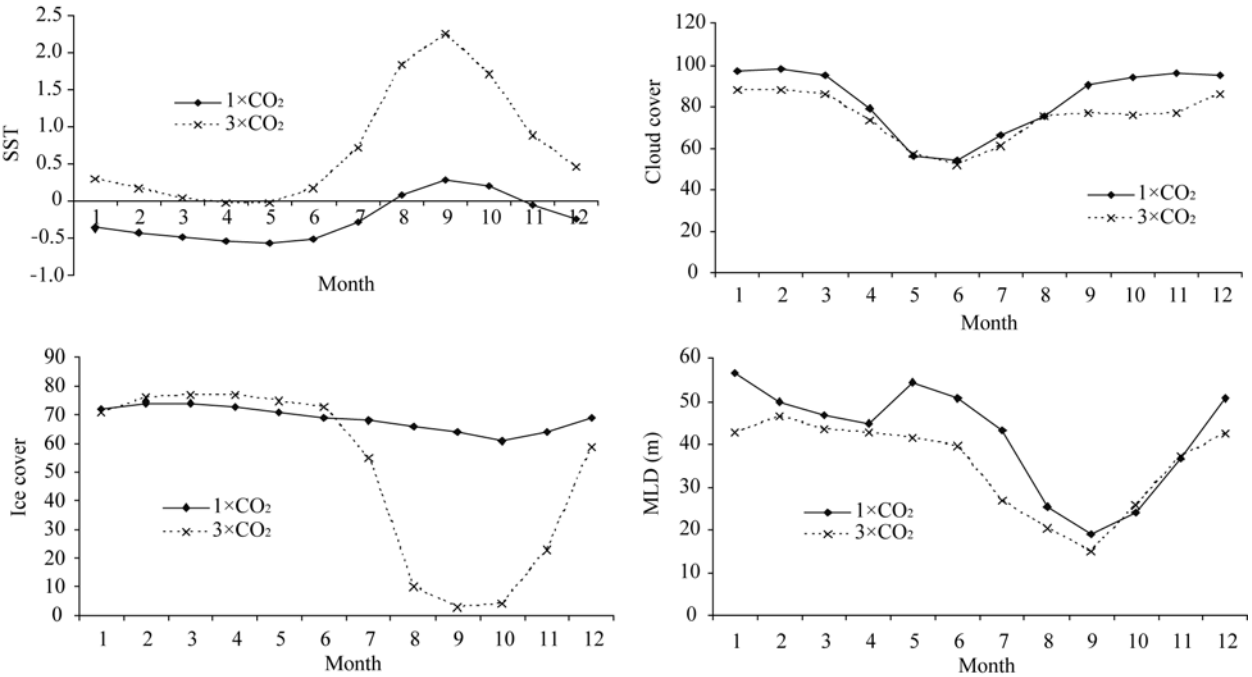

Fig.3 Comparison of the zonal transient climate data at 70–80°N in the two periods of 1×CO_2 and 3×CO_2

Hence, it is possible to quantify the flux of DMS from the oceans to investigate its impact on atmospheric chemistry and radiative transfer (Kettle et al., 2000). Because the DMS flux is related to the SST and wind speed (see Eq. 8), a change in temperature could significantly affect the regional DMS flux.

The DMS flux was calculated for ice-free water. A 5-year DMS flux time series was calculated using the parameters in Table 2. It is clear that the year 2002 saw the greatest DMS emission and 1999 saw the least DMS emission. This corresponds to the yearly ranking of CHL production (Qu et al. 2006), with greater CHL production resulting in greater DMS production. The SST and wind speed generally increased during the five years. It is notable that the year 1998 was the second most productive year after 2002. Considering the SST and wind speed did not significantly increase in 1998, the higher DMS flux may related to the ice cover being confined to the southern part of the region in that year.

Fig.4 shows changes between the two periods (from 1×CO_2 to 3×CO_2). The peak in the phytoplankton amount (P) shifts one month earlier in summer. The mean peak of the zooplankton amount (Z) increases from 0.8 to 1.7 and the peak period shifts 20 days ahead in September. The DMS flux increases from an average of 0.8 μmol m^{-2} d^{-1} to 1.8 μmol m^{-2} d^{-1} in the whole band and increased 6.6 μmol m^{-2} d^{-1} in September. The peak DMS flux is in September with only a small peak in spring (March to April). The annual DMS flux more than doubles from 175.4 to 360.5 μmol m^{-2} from 1×CO_2 to 3×CO_2.

Table 6 summarizes both the contemporary DMS and annual DMS flux (with no ice and with ice but using adjusted flux values for ice-free water) at 70–80°N. This significant change in DMS emission and aerosol production in the Arctic atmosphere could have a large impact on the regional polar energy budget and hence on the wider phenomenon of global warming.

The Arctic Ocean circulations with special characteristic of sea-ice coverage, low temperature and a long dark winter make for unique marine biology. The large area of Arctic sea ice that melts in spring can affect mixing in and nutrient-delivery to the euphotic zone; hence, there is a significant spring vernal bloom immediately after the ice cover begins melting. The ice algae contribute a high DMSP content and there is a high biomass of *Phaeocystis sp.* and *Emiliania huxleyi*, leading to production of large quantities of DMS. The maximum DMS production takes place during the declining phase of algal blooms (consistent with what was reported by Belviso et al. (2003)). The high interannual variations in CHL amount lead to high interannual variations in the DMS amount and DMS flux. The higher DMS flux and earlier DMS spring bloom in 1998 could be related to there being more ice cover (and hence more ice algae) in the southern part of the study region. Both a significant reduction in the sea-ice coverage in autumn and a shallower MLD in summer suggests that DMS flux could increase significantly in autumn within the next 80 years.

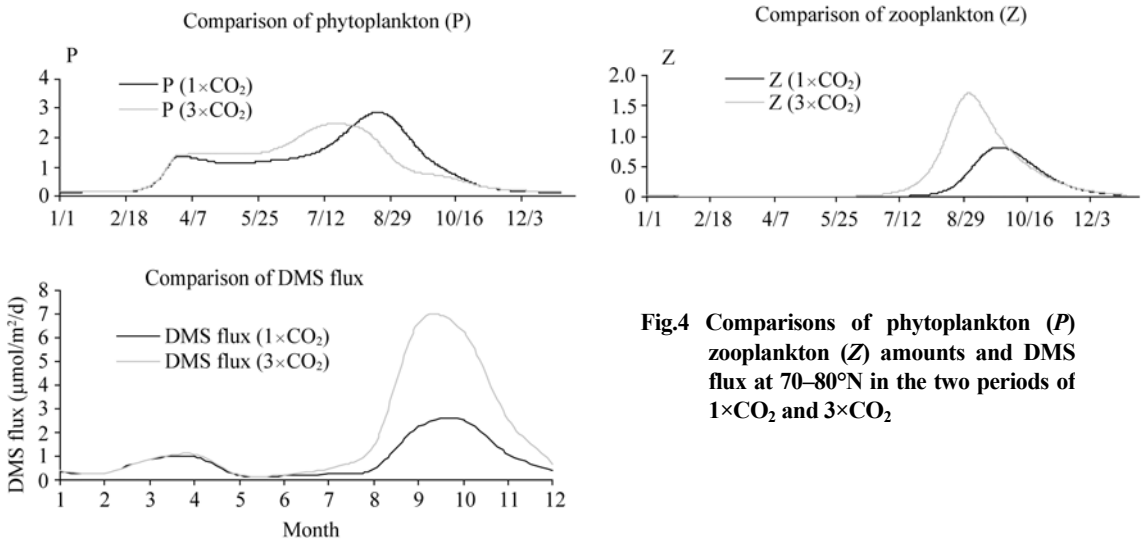

Fig.4 Comparisons of phytoplankton (*P*) zooplankton (*Z*) amounts and DMS flux at 70–80°N in the two periods of 1×CO_2 and 3×CO_2

Table 6 Comparison of predicted annual mean concentrations and fluxes of DMS for 70–80°N

Forcing Scenario	Mean DMS concentration (nmol/L)	Annual DMS flux (μmol m^{-2} a^{-1})	Annual DMS flux (After adjustment for ice) (μmol m^{-2} a^{-1})
Contemporary (30-35E)	6.3	2 227.7	1 265.2
GCM 1×CO_2	7.2	531.6	175.4
GCM 3×CO_2	7.6	590.4	360.5

5 CONCLUSION

In this paper, both satellite data and field data sets were used to calibrate a regional DMS production model. The GA proved an efficient tool in the multiple-parameter calibration task. Model simulations indicate significant interannual variation in the CHL amount leading to significant interannual variability in the observed and modeled production of DMS in the study region. The GCM-simulated physical forcings for the 70–80°N band of decreasing sea-ice coverage, significant increasing of the SST and a decreasing MLD are the main causes of a simulated annual DMS flux increase of more than 100% by the time of equivalent CO_2 tripling (in the year 2080). Such a large change would have a great impact on the Arctic energy budget and may offset the effects of anthropogenic warming that are amplified at polar latitudes. It is important to note that many of these physical changes will also promote similar perturbations for other biogenic species (Leck et al. 2004), some of which are now thought to be equally influential to the aerosol climate of the Arctic Ocean.

6 ACKNOWLEDGMENTS

The authors wish to thank Dr. Patricia A. Matrai for kindly providing the field data of the three ALV cruises (ALV is part of the Norwegian research programme “Arktisk lys og varme”), and we thank Dr. Paul Wassmann as Chief Scientist for organizing the cruises. The authors also wish to thank Dr. Roger A. Cropp for technical assistance. We thank the SeaWiFS Project (Code 970.2) and the Distributed Active Archive Centre (Code 902) at the Goddard Space Flight Centre, Greenbelt, MD 20771, for the production and distribution of the SeaWiFS data respectively. These activities are sponsored by the National Aeronautics and Space Administration (NASA) Mission to Planet Earth (http://seawifs.gsfc.nasa.gov). We thank the Reynolds/NCEP (National Centers for Environmental Prediction) in PO.DAAC Ocean ESIP Tool (POET) (http://podaac-esip.jpl.nasa.gov/poet/) for the SST and wind speed data. The Quikscat/SeaWinds and Advanced Very High Resolution Radiometer data were obtained from the NASA Physical Oceanography Distributed Active Archive Centre at the Jet Propulsion Laboratory/ California Institute of Technology (http://podaac.jpl.nasa.gov). The SSMI data were provided by the Defense Meteorological Satellite Program, National Oceanic and Atmospheric Administration (NOAA), United States Department of Commerce (http://www.ncdc.noaa.gov). The MLD data were taken from the NODC (National Oceanographic Data Center,

Levitus) World Ocean Atlas 1994 provided by the NOAA-CIRES(Cooperative Institute for Research in Environmental Sciences) Climate Diagnostics Centre, Boulder Colorado, (http://www.cdc.noaa.gov/). The World Ocean Atlas 1998 was supplied by the Ocean Climate Laboratory, National Oceanographic Data Centre, NOAA, United States Department of Commerce (http://www.nodc.noaa.gov). We thank Dr. David L. Carroll from CU Aerospace (An integrated aerospace company located near the southwest corner of the University of Illinois at Urbana-Champaign campus) for the genetic algorithm Fortran code. We thank Steven J. Worley from the Data Support Section, NCAR/SCD (National Center for Atmospheric Research's Scientific Computing Division) (http://www.dss.ucar.edu), for providing metrological data such as cloud cover. Finally, we gratefully acknowledge the financial assistance of an Australian Research Council Discovery Grant.

References

Archer S D, Gilbert F J, Nightingale P D, Zubkov M V, Taylor A H, Smith G C, Burkill P H. 2002. Transformation of dimethylsulphoniopropionate to dimethyl sulphide during summer in the North Sea with an examination of key processes via a modelling approach. *Deep-Sea Research Part I-Topical Studies in Oceanography*, **49**(15), 3 067-3 101.

Belviso A, Sciandra A, Copin-Montegut C. 2003. Mesoscale features of surface water DMSP and DMS concentrations in the Atlantic Ocean off Morocco and in the Mediterranean Sea. *Deep Sea Research, Part I: Tropical Studies in Oceanography*, **50**: 543-555.

Charlson R J, Lovelock J E, Andreae M O, Warren S G. 1987. Oceanic phytoplankton, atmospheric sulphur, cloud albedo and climate. *Nature*, **326**: 655-661.

Cropp R A. 2003. A biogeochemical modeling analysis of the potential for marine ecosystems to regulate climate by the production of dimethylsulphide, PhD thesis, School of Australian Environmental Studies, Griffith University: Brisbane. p. 280.

Dacey J W H, F A Howse, A F Michaels, Wakeham S G. 1998. Temporal variability of dimethylsulfide and simethylsulfoniopropionate in the Sargasso Sea. *Deep-Sea Research I*, **45**: 2 085-2 104.

Erickson D J, Ghan S J, Penner J E. 1990. Global ocean-to-atmosphere dimethyl sulfide flux, *J. Geophys. Res.*, **95**(D6): 7 543-7 552.

Gabric A J, Murray N, Stone L, Kohl M. 1993. Modeling the Production of Dimethylsulfide During a Phytoplankton Bloom. *Journal of Geophysical Research*, **98**(C12): 22 805-22 816.

Gabric A J, Ayers G P, Sander G C. 1995. Independent marine and atmospheric model estimates of the sea-air flux of dimethylsulfide in the Southern Ocean. *Geophysical Research Letters*, **22**(24): 3 521-3 524.

Gabric A J, Whetton P H, Boers R, Ayers G P. 1998. The impact of simulated climate change on the sir-sea flux of dimethylsulphide in the subantarctic Southern Ocean. *Tellus*. **50B**: 388-399.

Gabric A J, Matrai P A. 1999. Modeling the production and cycling of dimethylsulphide during the vernal bloom in the Barnents Sea. *Tellus*, **51B**: 919-937.

Gabric A J, Whetton P, Cropp R. 2001. Dimethylsulphide production in the Subantarctic Southern Ocean under enhanced greenhouse conditions. *Tellus*, **53B**: 273-287.

Gabric A J, Cropp R, Ayers G P, McTaubsh G, Braddock R. 2002. Couple between cycles of phytoplankton biomass and aerosol optical depth as derived from SeaWiFS time series in the Subantarctic Southern Ocean. *Geophysical Research Letter*, **29**(7), (16-1)-(16-4).

Gabric A J, Cropp R, Hirst T, Marchant H. 2003. The sensitivity of dimethyl sulfide producion to simulated climate change in the Eastern Antarctic Southern Ocean. *Tellus*, **55B**: 966-981.

Gabric A J, Qu B, Matrai P A , Hirst A C. 2005. The simulated response of dimethylsulphide production in the Arctic Ocean to global warming. *Tellus*, **57B**, 391-403.

Gage D A, Phodes D, Nolte K D, Hicks W A, Leustek T, Cooper A J L, Hanson A D. 1997. A new routh for synthesis of dimethylsulphoniopropionate in marine algae. *Nature*, **387**: 891-894.

Gordon H G, O'Farrell S P. 1997. Transient climate change in the CSIRO coupled model with dynamic sea ice. *Mon. Weather Rev.*, **125**: 875-907.

Holland, John H. 1975. Adaptation in Natural and Artificial Systems, University of Michigan Press, Ann Arbor MI.

Holland M M, Bitz C M, Tremblay B. 2006, Future abrupt reductions in the summer Arctic sea ice, *Geophys. Res. Lett.*, **33**: L23503. doi:10.1029/2006GL028024.

Kettle A J, Andreae M O. 2000. Flux of dimethylsulfide from the ocean: A comparison of updated data sets and flux models. *Journal of Geophysical Research*. **105**(D22): 26 793-26 808.

Kiene R P, Bates T S. 1990. Biological removal of dimethylsulphide from sea water. *Nature*, **345**: 702-705.

Kirst G O, Thiel C, Wolff H, Nothnagel J, Wanzek M, Ulmke R. 1991. Dimethylsulfoniopropionate (Dmsp) in Ice-Algae and Its Possible Biological Role. *Marine Chemistry*, **35**(1-4): 381-388.

Kloster S, Six K D, Feichter J. 2007. Response of dimethylsulfide (DMS) in the ocean and atmosphere to global warming, *J. Geophys. Res.*, **112**, G03005, doi:10.1029/2006JG000224.

Lawrence M G. 1993. An empirical analysis of the strength of the phytoplankton-dimethylsulfide-cloud-climate feedback cycle. *Journal of Geophysical Research*, **98**: 20 663-20 673.

Leck C, Persson C. 1996. Seasonal and short-term variability in dimethyl sulfide sulfur dioxide and biogenic sulfur and

sea salt aerosol particles in the arctic marine boundary layer during summer and autumn. *Tellus*, **48B**: 272-299.

Leck C, Tjernström M, Matrai P, Swietlicki E, Bigg E K. 2004. Can Marine Micro-organisms Influence Melting of the Arctic pack Ice? *Eos. Trans.,* AGU, **85**(3): 25-36.

Levasseur M, Gosselin M, Michaud S. 1994. A new source of dimethylsulfide (DMS) for the Arctic atmosphere: ice diatoms. *Mar. Biol.,* **121**:381-387.

Liss P S, Merlivat L. 1986. Air-sea gas exchange rates: Introduction and synthesis. *In*: The role of air-sea exchange in geochemical cycling, ed. P. Buat-Menard. Reidel, Hingham, MA. 113-127.

Lovelock J E, Maggs R J, Rasmussen R A. 1972. Atmospheric dimethylsulphide and the natural sulphur cycle. *Nature*, **237**: 452-453.

Matrai P A, Vernet M. 1997. Dynamics of the vernal bloom in the marginal ice zone of the Barents Sea: Dimethylsulfide and dimethysulfoniopropionate budgets. *Journal of Geophysical Research-Ocean*, **102**(C10), 22 965-22 979.

Moline M A, Karnovsky N J, Brown Z. 2008. High latitude changes in ice dynamics and their impact on polar marine ecosystems. *Year in Ecology and Conservation Biology*. **1 134**: 267-319.

Moloney C L, Bergh M O, Field J G, Newell R C. 1986. The effect of sedimentation and microbial nitrogen regeneration in a plankton community: a simulation investigation. *Journal of plankton research*, **8**(3), 427-445.

Qu B, Gabric A J, Matrai P A. 2006. The satellite-derived distribution of chlorophyll-*a* and its relation to ice cover, radiation and sea surface temperature in the Barents Sea. *Polar Biology*, **29**: 196-210.

Serreze M C, Francis J A. 2006. The arctic amplification debate. *Climatic Change*, **76**(3-4): 241-264.

Treffeisen R, Rinke A, Fortmann M. 2005. A case study of the radiative effects of Arctic aerosols in March 2000. *Atmospheric Environment*, **39**(5), 899-911.